

On the Mechanism of Action of Fullerene Derivatives in Superoxide Dismutation

Sílvia Osuna,^[a] Marcel Swart,^{*,[a, b]} and Miquel Solà^{*,[a]}

Abstract: We have studied the mechanism of the antioxidant activity of C₆₀ derivatives at the BP86/TZP level with inclusion of solvent effects (DMSO) by using the COSMO approach. The reaction studied here involves degradation of the biologically relevant superoxide radical (O₂^{•-}), which is linked to tissue damage in several human disorders. Several fullerene derivatives have experimentally been shown to be protective in cell culture and animal models of injury, but precisely how these compounds protect biological systems is still unknown. We have investigated the activity of tris-malonyl C₆₀ (also

called C₃), which efficiently removes the superoxide anion with an activity in the range of several biologically effective, metal-containing superoxide dismutase mimetics. The antioxidant properties of C₃ are attributed to the high affinity of C₆₀ to accept electrons. Our results show that once the superoxide radical is in contact with the surface of C₃, its unpaired electron is transferred to the fullerene. This pro-

cess, which converts the damaging O₂^{•-} to neutral oxygen O₂, is the rate-determining step of the reaction. Afterwards, another superoxide radical reacts with C₃^{•-} to form hydrogen peroxide and in the process takes up the additional electron that was transferred in the first step. The overall process is clearly exothermic and, in general, involves reaction steps with relatively low activation barriers. The capability of C₃ to degrade a highly reactive oxygen species that is linked to several human diseases is of immediate interest for future applications in the field of biology and medicine.

Keywords: antioxidants • density functional calculations • fullerenes • radicals • radical reactions

Introduction

In living beings there exists a delicate equilibrium between the biological processes responsible for the production of reactive oxygen species (ROS) and those for their removal, which when unbalanced may result in oxidative stress. The most prominent ROS is the superoxide radical (O₂^{•-}), which is basically formed due to errors in oxidative phosphorylation in mitochondria, and the hydroxyl radical (OH[•]). Hydrogen peroxide (H₂O₂) and peroxynitrite (ONOO⁻),

formed during reaction of superoxide with nitric oxide (NO), can also be involved in oxidative processes.^[1] Biological enzymatic defense mechanisms such as superoxide dismutases (SODs), glutathione peroxidase and catalase, and nonenzymatic mechanisms such as vitamin E (α -tocopherol), ascorbic acid, and glutathione are responsible for controlling the levels and activity of ROS.^[2] All cellular biomacromolecules (lipids, sugars, proteins, and DNA) are vulnerable to reaction with ROS, and generated secondary products can be even more prejudicial than the initial ROS. The highest concentration of oxygen is found in the central nervous system, and this, together with the low levels of antioxidant molecules and the high content of polyunsaturated lipids, makes the brain extremely vulnerable to oxidation. Consequently, it is believed that oxidative stress has an important role in most neurodegenerative disorders.^[3] Accumulation of oxidative damage may be involved in the ageing process, and there is irrefutable evidence that oxidative stress of some components is observed in neurodegenerative diseases such as amyotrophic lateral sclerosis (ALS), Alzheimer's disease, Parkinson's disease, and Huntington disorders.^[3,4]

Among ROS species, the superoxide radical (O₂^{•-}) was found to be linked to tissue damage in human disease states

[a] S. Osuna, Prof. Dr. M. Swart, Prof. Dr. M. Solà
Institut de Química Computacional and Departament de Química
Universitat de Girona, Campus Montilivi
17071 Girona (Spain)
E-mail: miquel.sola@udg.edu

[b] Prof. Dr. M. Swart
Institució Catalana de Recerca i Estudis Avançats (ICREA)
Pg. Lluís Companys 23, 08010 Barcelona (Spain)
E-mail: marcel.swart@icrea.es

Supporting information for this article (all schemes and figures in color; Table S1 listing BP86/TZP optimized Cartesian xyz coordinates of all analyzed species) is available on the WWW under <http://dx.doi.org/10.1002/chem.200902728>.

such as stroke, cancer, and inflammatory diseases.^[5–7] Because of this toxicity of superoxide, a defense mechanism has evolved in organisms from bacteria to mammals that involves SOD enzymes to detoxify the superoxide radical. However, these antioxidant defenses, including the superoxide dismutases, may be overwhelmed by abundant ROS, and tissue damage results. Therefore, either increasing the SOD activity or administering a SOD mimetic could attenuate tissue injury in neurodegenerative disorders and inflammatory diseases.^[8]

Several fullerene derivatives were shown to be protective against oxidative stress in cell culture and animal models of injury, including bacterial sepsis,^[9] degeneration of dopaminergic neurons in Parkinson's disease,^[10–12] and nervous system ischemia.^[13,14] Among them, the most widely studied is tris-malonyl C₆₀ (also called C₃, see Figure 1). Experimentally, the cyclopropanation of C₆₀ with diethyl bromomalonate in toluene with NaH as auxiliary base proceeds smoothly at room temperature^[15,16] and exclusively at bonds situated between two hexagonal rings ([6,6] bonds). The synthesis of bis-adducts and tris-adducts is also possible by applying the same reaction conditions to mono- and bis-adducts, respectively.^[17] Tris-malonyl compounds with C₃ and D₃ symmetry are produced in a yield of 40%.^[17]

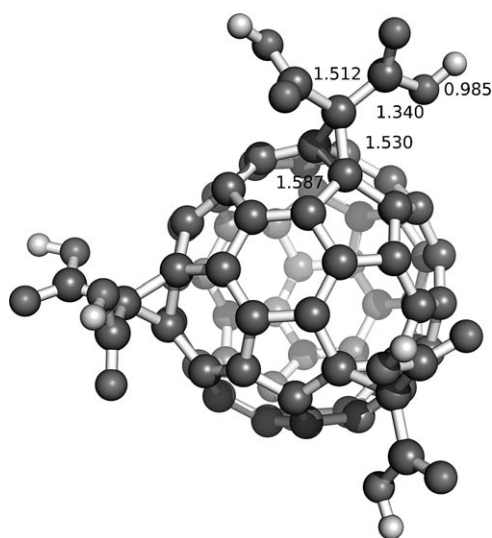


Figure 1. BP86/TZP-optimized geometry including DMSO as solvent of the tris-malonyl C₆₀ compound known as C₃. The three malonyl groups are attached to the fullerene compound through [6,6] bonds.

The C₃ compound can efficiently remove the superoxide anion, albeit at a slower rate than enzymes present in living beings such as SOD1 (a superoxide dismutase primarily present in the cytoplasm) or SOD2 (which is restricted to mitochondria). Nevertheless, the rate of removal is well within the range of several biologically effective, metal-containing SOD mimetics.^[18] Moreover, the *in vivo* activity of C₃ was also satisfactorily tested in mice, with a similar activity to that observed for manganese superoxide dismutase

(MnSOD) mimetics.^[18] Structure–function studies on these carboxyfullerenes indicated that the antioxidant properties of the different compounds depend on redox behavior, charge, size, shape, and hydrophobicity.^[19] Higher antioxidant activity is found for anionic fullerenes than for comparable cationic compounds.^[19] Moreover, the reactivity of carboxyfullerenes towards superoxide was found to be related to the dipole moment, which is clearly influenced by the number of carboxyl groups present and their position in the fullerene compound.^[20] For instance, the antioxidant activity of tris-malonyl carboxyfullerene with C₃ symmetry was reported to be higher than that of its D₃-symmetric counterpart.^[10] Liu et al. found that the SOD activity of different carboxyfullerenes was dependent on their reduction potentials: the higher the reduction potential the higher the SOD dismutation activity.^[21] They observed that the molecular structure of the fullerene derivative is important, too, as fullerene derivatives with similar reduction potentials but substantially different architectures exhibit completely distinct antioxidant activities. They recently also evaluated the antioxidant activity of several mono-adducts (i.e., only one malonyl unit is attached to the fullerene surface) and found a higher activity compared to the archetypal compound C₃.^[21] Moreover, mono-adducts are more stable, less toxic,^[22] and can be produced in higher yields. Other related compounds, such as fullerene-containing peptide nanoparticles obtained through self-assembly, were found to exhibit antioxidant activity as well.^[23] The SOD removal activities of the carboxyfullerene C₆₀[C(COOH)₂]₂, the hydroxyfullerene C₆₀(OH)₂₂, and the endohedral gadolinium-based C₈₂ hydroxyfullerene Gd@C₈₂(OH)₂₂ were compared by Yin and co-workers.^[24] The highest activity was found for Gd@C₈₂(OH)₂₂ followed by C₆₀(OH)₂₂ and C₆₀[C(COOH)₂]₂.

Several biomedical studies were performed in which the antioxidant capability of carboxyfullerene C₃ or a related compound was studied in detail. C₃ treatment of mice that lack mitochondrial MnSOD increased the lifespan by 300%, which supports the hypothesis that C₃ is localized in mitochondria and acts as a biologically effective SOD mimetic.^[18] The administration of carboxyfullerenes to mice starting at middle age reduced age-associated oxidative stress and mitochondrial radical production in addition to an increase in lifespan.^[25] Moreover, treated mice were found to improve in learning and memory tasks. The latter results are extremely relevant, as administration of fullerene derivatives seems to improve age-related cognitive impairment in mammals.

The C₃ compound also exhibits cytochrome c peroxidase-like activity.^[26] Carboxyfullerenes were found to protect against oxidative stress induced apoptosis (cellular death) in human peripheral blood mononuclear cells and in rat cerebellum granule cells.^[27,28] Infusion of iron(II) compounds in mice induced an increase in lipid peroxidation in a certain brain region called substantia nigra, and a decrease in dopamine content in the striatum area of the brain.^[11] Indeed, lipid peroxidation in Parkinson's patients is higher than that of control systems.^[29–31] Infusion of carboxyfullerene led to a

suppression of both lipid peroxidation and decreased dopamine content in the striatum in a dose-dependent manner. Therefore, C₃ and its derivatives may be novel candidates for treating neurodegenerative disorders like Parkinson's disease. The antioxidant effect in the prevention of lipid peroxidation induced by superoxide and hydroxyl radicals of C₃ was found to be slightly higher than that of vitamin E for liposoluble antioxidants.^[32] This compound may also be useful to treat other neurodegenerative disorders such as amyotrophic lateral sclerosis (ALS). Administration of C₃ to a mouse model of familial ALS retarded its death and motor deterioration.^[10] Wang and co-workers found that the administration of endohedral hydroxyfullerenes [Gd@C₈₂(OH)₂₂]_n to tumor-bearing mice efficiently restored their damaged liver and kidney.^[33] All parameters related to oxidative stress were restored to the normal levels after [Gd@C₈₂(OH)₂₂]_n administration.

The mechanism behind the antioxidant activity of C₃ and related compounds is still an open issue. Some studies have suggested that the oxidation of radical anions occurs due to the highly conjugated double-bond system of the fullerene structure, which is considered to be the main factor responsible for its antioxidant action.^[34] Moreover, the reactivity of C₆₀ towards radicals such as hydroxyl or alkoxy is clearly enhanced compared to planar aromatic compounds^[35] and products of C₆₀ reacting with hydroxyl,^[36] alkylperoxy, alkyl, and benzyl radicals^[37] have been experimentally detected. However, the mechanism of this superoxide removal still remains controversial. Dugan and co-workers proposed a catalytic superoxide dismutation mechanism based on experimental observations.^[18] Formation of a complex between C₃ and O₂^{•-} was also proposed.^[18,21] Liu et al. presented experimental evidence for a catalytic dismutation process in which the key steps of the reaction were oxidation of O₂^{•-} produced in an outer-sphere electron-transfer process and fullerene reduction.

As far as we know, there are no theoretical studies on the SOD dismutase mechanism involving carboxyfullerenes such as C₃. Although there is experimental evidence that carboxyfullerenes decrease ROS production, the mechanism of action in the dismutation process is still unclear. Thus, theoretical calculations could provide a deeper insight into the role of C₃ in superoxide removal. The promising results found in vivo and in vitro make these fullerene compounds extremely interesting for future medical progress. The understanding of the SOD removal mechanism could represent a big improvement to design new fullerene derivatives with improved antioxidant properties. The present computational work aims to study the antioxidant activity of C₃ type fullerenes in order to provide a better understanding of the mechanism of action of such a fundamental chemical process.

Computational Details

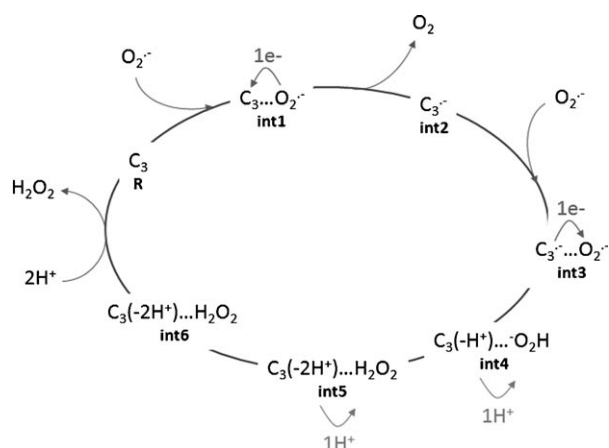
All DFT calculations were performed with the Amsterdam Density Functional (ADF) program^[38,39] and the related QUILD^[40,41] (QUantum-regions Interconnected by Local Descriptions). The molecular orbitals (MOs) were expanded in an uncontracted set of Slater-type orbitals (STOs) of triple- ζ (TZP) quality containing diffuse functions and one set of polarization functions. Core electrons (1s for 2nd period, 1s2s2p for 3rd and 4th periods) were not treated explicitly during the geometry optimizations (frozen-core approximation),^[39] as it was shown to have a negligible effect on the obtained geometries.^[42] An auxiliary set of s, p, d, f, and g STOs was used to fit the molecular density and to represent the Coulomb and exchange potentials accurately for each SCF cycle. Energies and gradients were calculated by using the local density approximation (Slater exchange and VWN correlation^[43]) with nonlocal corrections for exchange (Becke88)^[44] and correlation (Perdew86)^[45] included self-consistently (i.e., the BP86 functional). The latter method was shown to give deviations of less than 1 and 5 kcal mol⁻¹ as compared to CCSD(T)/aug-cc-pVDZ//MP2/aug-cc-pVDZ, respectively, for predicting the reaction and activation energies of free-radical substitution reactions.^[46,47] Solvent effects were taken into account in all geometry optimization and energy calculations by using the COSMO model, which was shown to perform well for solvation processes.^[48-52] The solvent used was the same as in the experiments, that is, dimethyl sulfoxide (DMSO).

The geometry optimizations and transition-state (TS) searches were performed with the QUILD^[40,41] program. QUILD constructs all input files for ADF, runs ADF, and collects all data; ADF is used only for the generation of the energy and gradients. Furthermore, the QUILD program uses improved geometry optimization techniques, such as adapted delocalized coordinates^[40] and specially constructed model Hessians with the appropriate number of eigenvalues.^[40] The latter is of particular use for TS searches. All TSs were characterized, by computing the analytical^[53] vibrational frequencies, to have one (and only one) imaginary frequency corresponding to the approach of the reacting molecules.

Results and Discussion

The mechanism of the superoxide removal involving fullerene derivative C₃ has been studied in detail. As mentioned in the introduction, C₃ has three malonyl groups attached to three [6,6] bonds of the C₆₀ surface (see Figure 1). The first objective was to find out which is the most favorable form of C₃ under the experimental conditions. Liu and co-workers used a large excess of KO₂ in DMSO containing 0.06% of water to test the antioxidant properties of different C₃-related compounds. Under these experimental conditions, we found that the fully protonated form of the carboxyl groups of C₃ is the most favorable configuration. In addition, optimization of several COOH configurations showed a slight preference for the isomer presented in Figure 1. Hence, SOD removal was studied only with this most favorable configuration of C₃. Scheme 1 shows the mechanism of superoxide removal induced by C₃, and Figure 2 the relative energies of the localized intermediate structures, TSs, and products for the whole process.

The first intermediate (**int1**) corresponds to interaction of the superoxide radical (O₂^{•-}) with the fullerene surface, six water molecules, and the potassium cation coming from the initial KO₂. The C₃, KO₂, and six H₂O molecules together with an additional O₂^{•-} species involved in the second part of the reaction constitute the model of the reaction consid-



Scheme 1. Schematic representation of the superoxide dismutase mechanism involving C_3 .

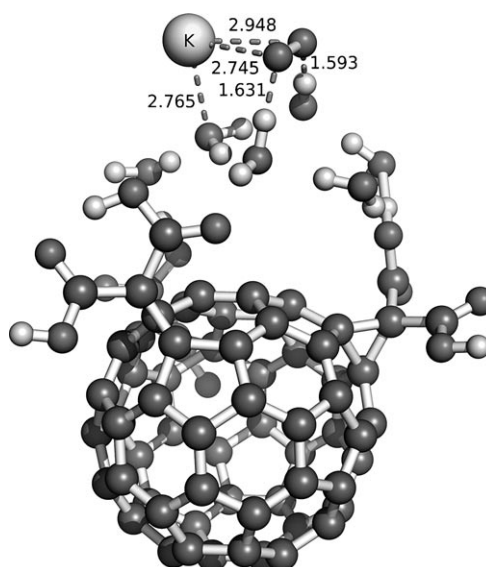


Figure 3. BP86/TZP-optimized geometry including DMSO as solvent of the first intermediate of the reaction (**int1**); relevant distances [\AA] are indicated by the dotted lines.

ered in the present mechanistic study. Note that the complete mechanism was studied with the potassium cation K^+ present, to represent the experimental conditions as well as possible. In the first intermediate, K^+ stabilizes the superoxide (with $K\cdots O^1$ and $K\cdots O^2$ distances of 2.9 and 2.7 \AA , respectively) and interacts with an oxygen atom of one of the water molecules (the $K\cdots O_{H_2O}$ 2.8 \AA , see Figure 3).

In this first step of the reaction, the transfer of the unpaired electron of the superoxide radical to C_3 has not occurred yet. Formation of the first intermediate **int1** repre-

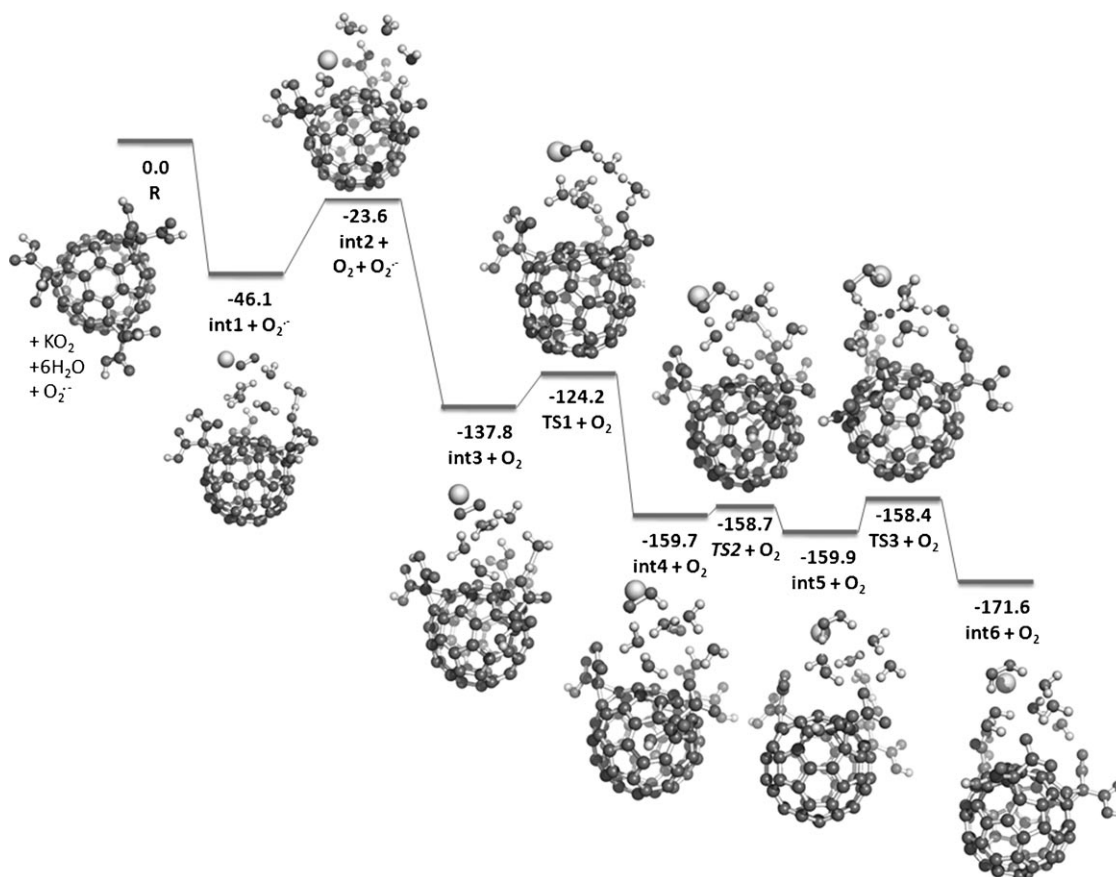


Figure 2. Reaction mechanism for SOD removal involving C_3 . All energies are expressed in kcal mol^{-1} .

sents an stabilization of $-46.1 \text{ kcal mol}^{-1}$ compared to the reactants ($\text{C}_3 + \text{KO}_2 + 6\text{H}_2\text{O}$). Once the unpaired electron of superoxide is transferred to C_3 in the second step, another intermediate (**int2**) is formed in which the superoxide radical has been transformed into a neutral oxygen molecule ($\text{C}_3 + \text{KO}_2 + 6\text{H}_2\text{O} \rightarrow \text{int2} + \text{O}_2$). This transfer of the unpaired electron from $\text{O}_2^{\cdot-}$ towards the carboxyfullerene has a reaction energy of $-23.6 \text{ kcal mol}^{-1}$. Although this electron transfer may have a TS which, in principle, could possibly be located by means of QM/MM strategies,^[54] searching for TS involving electron-transfer processes is not a straightforward procedure and may involve excited states of the **int1** species. Moreover, the geometrical changes induced by electron transfer are relatively minor, and the reaction barrier of the process is expected to be similar to the energy of **int2**. Therefore, the activation barrier for the process (**int1** \rightarrow **int2** + O_2) was estimated to be equal to the difference in energy between the two intermediates. Hence, the first step of the reaction has a substantial activation barrier of $22.5 \text{ kcal mol}^{-1}$ and is actually the rate-determining step of the reaction. As can be seen in Figure 4, the LUMO of free C_3 fullerene is 0.57 eV higher in energy than the SOMO and has about the same energy as the HOMO of free KO_2 .^[55] This is the main reason for the relatively small energy difference between **int1** (in which the electron has not yet been transferred) and **int2** (in which superoxide is converted to an oxygen molecule due to the redox process). This is in concordance with the experimental results by Liu and co-workers,^[21] who observed that C_3 derivatives with higher reduction potentials presented higher antioxidant activity. Given that a higher reduction potential corresponds to a greater affinity for accepting electrons, this implies more stabilized HOMO and LUMO. Stabilization of the LUMO of the carboxyfullerene facilitates electron transfer from the superoxide moiety to C_3 , as the difference in energy between LUMO (C_{60}) and HOMO (KO_2) becomes larger and more negative. The relatively high activation barrier found for the reduction/oxidation process (**int1** \rightarrow **int2** + O_2) for the archetypal C_3 compound studied here is consistent with the low antioxidant activity found experimentally,

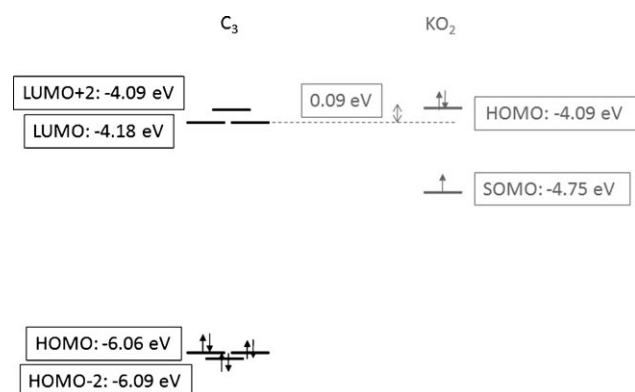


Figure 4. Diagram of the HOMOs and LUMOs of C_3 and KO_2 .

compared to other C_3 -related derivatives with higher reduction potentials.^[21]

The third intermediate (**int3**) is substantially more stable than the initial reactants ($-137.8 \text{ kcal mol}^{-1}$) and corresponds to the interaction between a second superoxide anion and the C_3 radical anion bearing an extra electron ($\text{C}_3^{\cdot-}$) that was transferred in the previous step of the reaction. The latter intermediate could represent either a singlet or a triplet spin state corresponding to antiparallel or parallel alignment of the unpaired electrons of the $\text{O}_2^{\cdot-}$ and $\text{C}_3^{\cdot-}$ radicals, respectively. Both possibilities have similar stabilities, as the unpaired electrons of the superoxide and fullerene are not in close contact (the difference in energy is only $0.1 \text{ kcal mol}^{-1}$). However, once the first proton is attached to the OO moiety (**int4**), which is accompanied by the transfer of an electron from the fullerene towards OO, the singlet state is clearly more stable than the triplet (the difference in energy then becomes $36.8 \text{ kcal mol}^{-1}$). This large singlet/triplet energy difference may be attributed to the preference of hydrogen peroxide (and related species) for a singlet ground state. At the same level of theory, the singlet spin state of an isolated H_2O_2 molecule is $37.2 \text{ kcal mol}^{-1}$ more stable than the triplet configuration. Interestingly, this spin-state splitting for an isolated hydrogen peroxide molecule is almost the same as that of the hydroperoxide species **int4**. Due to this strong preference for a singlet ground state, the whole mechanism was studied further for a singlet spin configuration.

We return now to the first proton-transfer step, in which a proton moves from one of the COOH groups of C_3 to the superoxide molecule. This step involves the presence of two interconnected water molecules (**TS1**) and has an activation barrier of $13.6 \text{ kcal mol}^{-1}$ compared to the previous intermediate **int3** (see Figures 2 and 5).

In **TS1**, the proton of one of the C_3 carboxyl groups is transferred to a water molecule (with $\text{O}_{\text{C}=\text{O}}-\text{H}$ and $\text{H}_{\text{COOH}}-\text{O}_{\text{H}_2\text{O}}$ distances of 1.297 and 1.357 \AA , respectively). At the same time, the same water molecule transfers another proton to a second water molecule ($d(\text{O}_{\text{H}_2\text{O}}^1-\text{H}_{\text{H}_2\text{O}}^1)$ and $d(\text{H}_{\text{H}_2\text{O}}^1-\text{O}_{\text{H}_2\text{O}}^2)$ are 1.191 and 1.255 \AA , respectively; see Figure 5). The latter water molecule interacts with superoxide with similar distances ($d(\text{O}_{\text{H}_2\text{O}}^2-\text{H}_{\text{H}_2\text{O}}^2)$ and $d(\text{H}_{\text{H}_2\text{O}}^2-\text{O}_{\text{O}_2^{\cdot-}})$ are 1.243 and 1.213 \AA , respectively). Therefore, this barrier involves simultaneous transfer of three protons.

After crossing this barrier, another intermediate is observed (**int4**) in which a single hydrogen atom is attached to the superoxide radical, that is, it corresponds to formation of the hydroperoxide anion (^-OOH). All attempts to find the subsequent transition state that might be surmounted (**TS2**) to finally obtain the hydrogen peroxide molecule (H_2O_2) were unfruitful. Therefore, we decided to perform a linear transit (LT) in five steps from **int4** to **int5** by simultaneously changing the lengths of five bonds (see Figure 6) which are involved in the transition between the reaction intermediates. The LT was carried out by using uniform steps for each of the five coordinates, that is, the coordinate values $R_{\text{linear transit}}^i$ at each step are given by Equation (1)

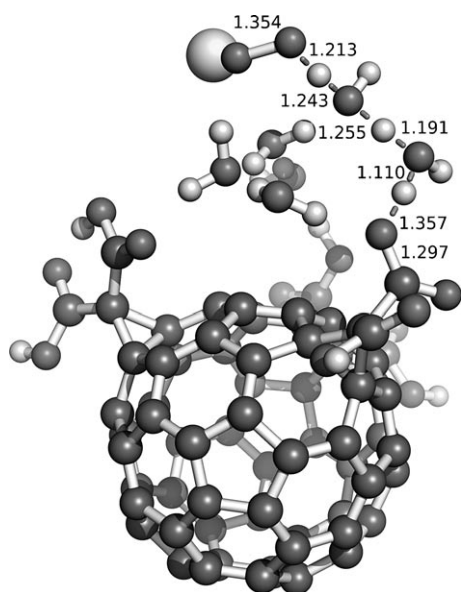


Figure 5. BP86/TZP-optimized geometry including DMSO as solvent of the transition state **TS1** that involves proton transfer from a C_3 carboxyl group towards the superoxide radical through two bridging water molecules; relevant distances [Å] are indicated by dotted lines.

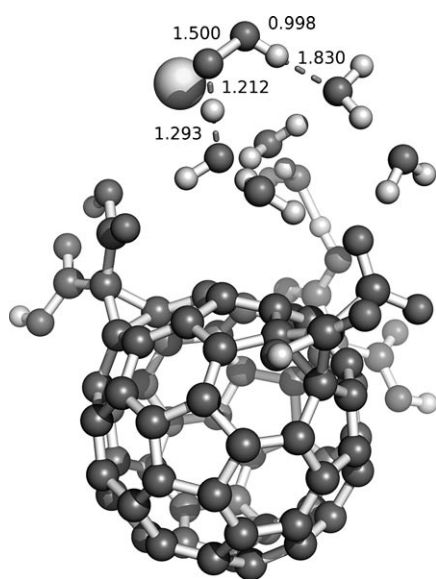


Figure 6. BP86/TZP-optimized geometry including DMSO as solvent of the maximum obtained in the linear transit from **int4** to **int5**. At each step of the LT the depicted distances have been modified in accordance with Equation (1). In this structure (presumably very similar to the real transition state **TS2**), the hydrogen peroxide molecule is formed by proton transfer from one of the closest water molecules; relevant distances [Å] are indicated by dotted lines.

$$R_{\text{lineartransit}}^i = R_{\text{int4}} + (i - 1) \frac{(R_{\text{int5}} - R_{\text{int4}})}{4} \quad (1)$$

in which $i=1-5$ and R_{int4} and R_{int5} are the coordinate values for **int4** and **int5**, respectively. The rest of the geometrical parameters were reoptimized at each step. In this linear

transit, a maximum in the energy profile was obtained that presents a very low barrier ($1.0 \text{ kcal mol}^{-1}$ with respect to **int4**). Although we were not able to fully locate the real TS for the process, the maxima detected in the LT gives a reasonable estimate for the activation barrier that must be surmounted to finally obtain **int5**. Note, however, that the difference in energy between **int4** and **int5** is only $0.2 \text{ kcal mol}^{-1}$. The optimized geometry for the maximum found in the LT (**TS2**), shown in Figure 6, involves only one hydrogen transfer from one of the water molecules close to the hydroperoxide anion, with O–H distances of approximately 1.2 Å .

After the formation of H_2O_2 in **int5**, a second proton transfer from the carboxyfullerene takes place in which the water molecule that gave up its proton to the hydrogen peroxide in **TS2** is now protonated again. This process involves three interconnected water molecules and corresponds to **TS3** (see Figure 7). The activation barrier of this process is only $1.5 \text{ kcal mol}^{-1}$ (referred to the previous intermediate **int5**). The distance between the hydrogen atom that is transferred either from the carboxyl group to a subsequent water molecule or from one water molecule to another is approximately 1.1 Å . However, the distance between the hydrogen atom that is being transferred and the final O atom to which it will be finally attached is approximately 1.3 Å in all cases. The main exception to this is the last proton transfer from the second to the third water molecule, for which the two distances are almost equal and approximately 1.2 Å (see Figure 7). In the last step of the reaction, the hydrogen peroxide formed interacts with C_3 and the K^+ cation (**int6**). The reaction energy of the latter intermediate is -171.6 kcal

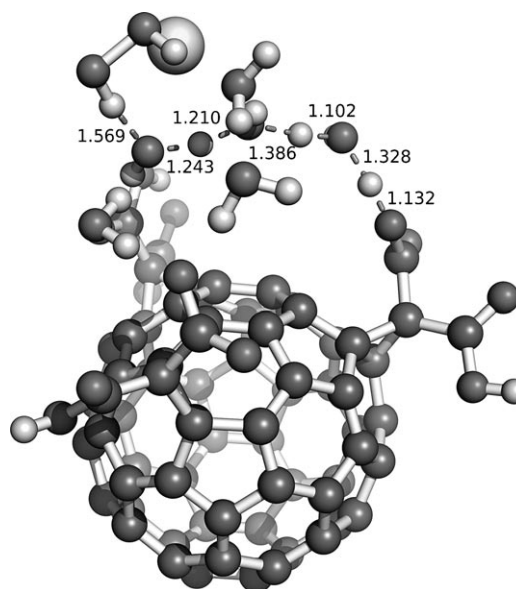


Figure 7. BP86/TZP-optimized geometry including DMSO as solvent of the transition state **TS3** that involves subsequent proton transfers from one protonated carboxyl group of C_3 to the deprotonated water molecule that in **TS2** transferred one of its hydrogen atoms to the hydroperoxide anion to form hydrogen peroxide; relevant distances [Å] are indicated by dotted lines.

mol^{-1} as compared to initial reactants ($\text{C}_3 + 6\text{H}_2\text{O} + \text{KO}_2 + \text{O}_2^{\cdot-}$).

At this point, the reaction could continue, as C_3 still has four protonated carboxyl groups, or C_3 could be reprotonated by taking up two external protons to recover the initial C_3 structure, which might be again involved in another antioxidant process. In the first case, six superoxide radicals could be converted to three oxygen molecules and three hydrogen peroxide molecules ($\text{C}_3 + 6\text{O}_2^{\cdot-} \rightarrow 3\text{O}_2 + 3\text{H}_2\text{O}_2 + \text{C}_3 - 6\text{H}^+$) by the same mechanism as described above, although probably with somewhat higher barriers for the proton transfers from the fullerene derivative to $\text{O}_2^{\cdot-}$. The reaction energy of the whole process is $-128.6 \text{ kcal mol}^{-1}$. Our theoretical calculations clearly indicate pronounced antioxidant character of C_3 and related compounds, as a single molecule is capable of converting six damaging superoxide radicals to oxygen and hydrogen peroxide. It was observed in some experimental studies that the presence of C_3 or related compounds not only decreased the superoxide concentration but also that of the harmful hydrogen peroxide formed during the SOD dismutation process.^[10,18] The results from this paper could be highly relevant to the final understanding of the antioxidant properties of C_3 and related compounds. The study of the first part of the mechanism, that is, the superoxide removal activity of C_3 acting as a SOD mimetic is crucial to understand further reactions of C_3 with byproducts of the superoxide removal process such as hydrogen peroxide.

Conclusions

Our theoretical calculations have shown that the superoxide removal mechanism involving fullerene compound C_3 is highly exothermic and the activation barriers that must be surmounted are, in general, low. The rate-determining step of the reaction is the redox process that transforms the superoxide radical into an oxygen molecule due to electron transfer of the unpaired electron of the superoxide radical to C_3 , the barrier of which basically depends on the LUMO energy of the fullerene. The lower the LUMO energy, the more favorable is the electronic transfer of the unpaired electron, as the difference in energy between the LUMO of C_3 and the HOMO of KO_2 is reduced or even negative. Hence, it is not surprising that, experimentally, C_3 -related compounds with different reduction potentials showed different antioxidant properties.^[21] After fullerene reduction, a second superoxide radical can react with the resulting $\text{C}_3^{\cdot-}$ radical by removing the extra electron and forming hydrogen peroxide H_2O_2 . This step involves the deprotonation of two of the six carboxyl groups of C_3 . The process is substantially exothermic and all activation barriers that must be surmounted are low. The first proton transfer (**TS1**) has a reaction barrier of 13 kcal mol^{-1} , whereas the remainder of the transition states (**TS2** and **TS3**) that lead to hydrogen peroxide formation have activation barriers of less than $1.6 \text{ kcal mol}^{-1}$. This capability of C_3 to remove highly reac-

tive oxygen species linked to several human diseases is extremely interesting for future applications of these compounds in the fields of biology and medicine.

Acknowledgements

This study was financially supported by the Spanish MICINN research projects CTQ2008-03077/BQU and CTQ2008-06532/BQU, the DURSI project nr. 2009SGR637, and the MICINN fellowship no. AP2005-2992. The authors acknowledge the computer resources, technical expertise, and assistance provided by the Barcelona Supercomputing Center—Centro Nacional de Supercomputación.

- [1] J. M. Onorato, S. R. Thorpe, J. W. Baynes, *Ann. N.Y. Acad. Sci.* **1998**, *854*, 277–290.
- [2] I. F. Benzie, *Int. J. Food Sci. Nutr.* **1996**, *47*, 233–261.
- [3] L. M. Sayre, G. Perry, M. A. Smith, *Chem. Res. Toxicol.* **2008**, *21*, 172–188.
- [4] M. Dib, C. Garrel, A. Favier, V. Robin, C. Desnuelle, *J. Neurol.* **2002**, *249*, 367–374.
- [5] I. Fridovich, *Ann. N.Y. Acad. Sci.* **1999**, *893*, 13–18.
- [6] H. Muramatsu, K. Kogawa, M. Tanaka, K. Okumura, Y. Nishihori, K. Koike, T. Kuga, Y. Niitsu, *Cancer Res.* **1995**, *55*, 6210–6214.
- [7] D. Salvemini, D. P. Riley, S. Cuzzocrea, *Nat. Rev. Drug Discovery* **2002**, *1*, 367–374.
- [8] A. D. Ross, H. Sheng, D. S. Warner, C. A. Piantadosi, I. Batinić-Haberle, B. J. Day, J. D. Crapo, *Free Radical Biol. Med.* **2002**, *33*, 1657–1669.
- [9] N. Tsao, T. Y. Luh, C. K. Chou, J. J. Wu, Y. S. Lin, H. Y. Lei, *Antimicrob. Agents Chemother.* **2001**, *45*, 1788–1793.
- [10] L. L. Dugan, E. G. Lovett, K. L. Quick, J. Lotharius, T. T. Lin, K. L. O'Malley, *Parkinsonism Relat. Disord.* **2001**, *7*, 243–246.
- [11] A. M. Lin, B. Y. Chyi, S. D. Wang, H. H. Yu, P. P. Kanakamma, T. Y. Luh, C. K. Chou, L. T. Ho, *J. Neurochem.* **1999**, *72*, 1634–1640.
- [12] J. Lotharius, L. L. Dugan, K. L. O'Malley, *J. Neurosci.* **1999**, *19*, 1284–1293.
- [13] L. L. Dugan, D. M. Turetsky, C. Du, D. Lobner, M. Wheeler, C. R. Almlı, C. K. Shen, T. Y. Luh, D. W. Choi, T. S. Lin, *Proc. Natl. Acad. Sci. USA* **1997**, *94*, 9434–9439.
- [14] S. S. Huang, S. k. Tsai, C. L. Chih, L. Y. Chiang, H. M. Hsieh, C. M. Teng, M. C. Tsai, *Free Radical Biol. Med.* **2001**, *30*, 643–649.
- [15] A. Hirsch, M. Brettreich, *Fullerenes: Chemistry and Reactions*, Wiley-VCH, Weinheim, **2004**.
- [16] C. Bingel, *Chem. Ber.* **1993**, *126*, 1957–1959.
- [17] A. Hirsch, I. Lamparth, H. R. Karfunkel, *Angew. Chem.* **1994**, *106*, 453–455; *Angew. Chem. Int. Ed. Engl.* **1994**, *33*, 437–438.
- [18] S. S. Ali, J. I. Hardt, K. L. Quick, J. S. Kim-Han, B. F. Erlanger, T. T. Huang, C. J. Epstein, L. L. Dugan, *Free Radical Biol. Med.* **2004**, *37*, 1191–1202.
- [19] P. Witte, F. Beuerle, U. Hartnagel, R. Lebovitz, A. Savouchkina, S. Sali, D. Guldi, N. Chronakis, A. Hirsch, *Org. Biomol. Chem.* **2007**, *5*, 3599–3613.
- [20] S. S. Ali, J. I. Hardt, L. L. Dugan, *Nanomedicine* **2008**, *4*, 283–294.
- [21] G. F. Liu, M. Filipovic, I. Ivanovic-Burmazovic, F. Beuerle, P. Witte, A. Hirsch, *Angew. Chem.* **2008**, *120*, 4055–4058; *Angew. Chem. Int. Ed.* **2008**, *47*, 3991–3994.
- [22] F. Beuerle, P. Witte, U. Hartnagel, R. Lebovitz, C. Parnig, A. Hirsch, *J. Exp. Nanosci.* **2007**, *2*, 147–170.
- [23] N. Higashi, T. Shosu, T. Koga, M. Niwa, T. Tanigawa, *J. Colloid Interface Sci.* **2006**, *298*, 118–123.
- [24] J. J. Yin, F. Lao, P. P. Fu, W. G. Wamer, Y. Zhao, P. C. Wang, Y. Qiu, B. Sun, G. Xing, J. Dong, X. J. Liang, C. Chen, *Biomaterials* **2009**, *30*, 611–621.
- [25] K. L. Quick, S. S. Ali, R. Arch, C. Xiong, D. Wozniak, L. L. Dugan, *Neurobiol. Aging* **2008**, *29*, 117–128.

- [26] K. Okuda, T. Mashino, M. Hirobe, *Bioorg. Med. Chem. Lett.* **1996**, *6*, 539–542.
- [27] M. Bisaglia, B. Natalini, R. Pellicciari, E. Straface, W. Malorni, C. Monti, D. Franceschi, G. Schettini, *J. Neurochem.* **2000**, *74*, 1197–1204.
- [28] D. Monti, L. Moretti, S. Salvioli, E. Straface, W. Malorni, R. Pellicciari, G. Schettini, M. Bisaglia, C. Pincelli, C. Fumelli, M. Bonafè, C. Franceschi, *Biochem. Biophys. Res. Commun.* **2000**, *277*, 711–717.
- [29] D. T. Dexter, A. E. Holley, W. D. Flitter, T. F. Slater, F. R. Wells, S. E. Daniel, A. J. Lees, P. Jenner, D. C. Marsden, *Mov. Disord.* **1994**, *9*, 92–97.
- [30] E. C. Hirsch, *Eur. Neurol.* **1993**, *33*, 52–59.
- [31] E. Sofic, W. Paulus, K. Jellinger, P. Riederer, M. B. H. Youdim, *J. Neurochem.* **1991**, *56*, 978–982.
- [32] I. C. Wang, L. A. Tai, D. D. Lee, P. P. Kanakamma, C. K. F. Shen, T.-Y. Luh, C. H. Cheng, K. C. Hwang, *J. Med. Chem.* **1999**, *42*, 4614–4620.
- [33] J. Wang, C. Chen, B. Li, H. Yu, Y. Zhao, J. Sun, Y. Li, G. Xing, H. Yuan, J. Tang, Z. Chen, H. Meng, Y. Gao, C. Ye, Z. Chai, C. Zhu, B. Ma, X. Fang, L. Wan, *Biochem. Pharmacol.* **2006**, *71*, 872–881.
- [34] S. S. Krusic, E. Wasserman, P. N. Keizer, J. R. Morton, K. F. Preston, *Science* **1991**, *254*, 1183–1185.
- [35] R. C. Haddon, *J. Am. Chem. Soc.* **1990**, *112*, 3385–3389.
- [36] R. V. Bensasson, M. Brettreich, J. Frederiksen, H. Gottinger, A. Hirsch, E. J. Land, S. Leach, D. J. McGarvey, H. Schonberger, *Free Radical Biol. Med.* **2000**, *29*, 26–33.
- [37] P. Krusic, E. Wasserman, B. A. Parkinson, B. Malone, E. R. J. Holler, *J. Am. Chem. Soc.* **1991**, *113*, 6274–6275.
- [38] ADF, E. J. Baerends, J. Autschbach, A. Bérces, F. M. Bickelhaupt, C. Bo, P. L. de Boeij, P. M. Boerrigter, L. Cavallo, D. P. Chong, L. Deng, R. M. Dickson, D. E. Ellis, L. Fan, T. H. Fischer, C. Fonseca Guerra, S. J. A. van Gisbergen, J. A. Groeneveld, O. V. Gritsenko, M. Grüning, F. E. Harris, P. van den Hoek, C. R. Jacob, H. Jacobsen, L. Jensen, G. van Kessel, F. Kootstra, E. van Lenthe, D. A. McCormack, A. Michalak, J. Neugebauer, V. P. Osinga, S. Patchkovskii, P. H. T. Philipsen, D. Post, C. C. Pye, W. Ravenek, P. Ros, P. R. T. Schipper, G. Schreckenbach, J. G. Snijders, M. Solà, M. Swart, D. Swerhone, G. te Velde, P. Vernooijs, L. Versluis, L. Visscher, O. Visser, F. Wang, T. A. Wesolowski, E. van Wezenbeek, G. Wiesenecker, S. K. Wolff, T. K. Woo, A. L. Yakovlev, T. Ziegler, SCM, Amsterdam, **2006**.
- [39] G. te Velde, F. M. Bickelhaupt, E. J. Baerends, C. Fonseca Guerra, S. J. A. van Gisbergen, J. G. Snijders, T. Ziegler, *J. Comput. Chem.* **2001**, *22*, 931–967.
- [40] M. Swart, F. M. Bickelhaupt, *Int. J. Quantum Chem.* **2006**, *106*, 2536–2544.
- [41] M. Swart, F. M. Bickelhaupt, *J. Comput. Chem.* **2008**, *29*, 724–734.
- [42] M. Swart, J. G. Snijders, *Theor. Chem. Acc.* **2003**, *110*, 34–41.
- [43] S. H. Vosko, L. Wilk, M. Nusair, *Can. J. Phys.* **1980**, *58*, 1200–1211.
- [44] A. D. Becke, *Phys. Rev. A* **1988**, *38*, 3098–3100.
- [45] J. P. Perdew, *Phys. Rev. B* **1986**, *33*, 8800–8802.
- [46] M. Swart, M. Solà, F. M. Bickelhaupt, *J. Comput. Chem.* **2007**, *28*, 1551–1560.
- [47] H. Matsubara, S. M. Horvat, C. H. Schiesser, *Org. Biomol. Chem.* **2003**, *1*, 1199–1203.
- [48] A. Klamt, G. Schüürmann, *J. Chem. Soc. Perkin Trans. 1* **1993**, *2*, 799–805.
- [49] C. C. Pye, T. Ziegler, *Theor. Chem. Acc.* **1999**, *101*, 396–408.
- [50] S. Osuna, M. Swart, E. J. Baerends, F. M. Bickelhaupt, M. Solà, *ChemPhysChem* **2009**, *10*, 2955–2967.
- [51] M. Swart, E. Rösler, F. M. Bickelhaupt, *Eur. J. Inorg. Chem.* **2007**, 3646–3654.
- [52] T. van der Wijst, C. Fonseca Guerra, M. Swart, F. M. Bickelhaupt, B. Lippert, *Angew. Chem.* **2009**, *121*, 3335–3337; *Angew. Chem. Int. Ed.* **2009**, *48*, 3285–3287.
- [53] S. K. Wolff, *Int. J. Quantum Chem.* **2005**, *104*, 645–659.
- [54] V. Guallar, F. Wallrapp, *J. R. Soc. Interface* **2008**, *5*, 233–239.
- [55] The superoxide unit in KO_2 (K^+O_2^-) has the same orbitals and occupations as the O_2 molecule but with one additional electron in a π^* orbital. Therefore, one of these π^* orbitals is a SOMO and the other π^* orbital with somewhat higher energy is the HOMO. Like NO , O_2^- has intrinsic multideterminant character. Unfortunately, the size of the systems studied prevents the use of multiconfigurational methods in this study.

Received: October 4, 2009
Published online: January 29, 2010